Continuous HMM-Based Seismic-Event Classification at Deception Island, Antarctica

M. C. Benítez, *Member, IEEE*, Javier Ramírez, José C. Segura, *Senior Member, IEEE*, Jesús M. Ibáñez, Javier Almendros, Araceli García-Yeguas, and Guillermo Cortés

***Abstract*—This paper shows a complete seismic-event classification and monitoring system that has been developed based on the seismicity observed during three summer Antarctic surveys at the Deception Island Volcano, Antarctica. The system is based on the state of the art in hidden Markov modeling (HMM) techniques successfully applied to other scenarios. A database that contains a representative set of different seismic events including volcano-tectonic earthquakes, long period (LP) events, volcanic tremor, and hybrid events that were recorded during the 1994–1995 and 1995–1996 seismic surveys was collected for training and testing. Simple left-to-right HMMs and multivariate Gaussian probability density functions with a diagonal covariance matrix were used. The feature vector consists of the log-energies of a filter bank that consists of 16 triangular weighting functions that were uniformly spaced between 0 and 20 Hz and the first- and second-order derivatives. The system is suitable to operate in real time, and its accuracy for this task is about 90%. On the other hand, when the system was tested with a different data set including mainly LP events that were registered during several seismic swarms during the 2001–2002 field survey, more than 95% of the recognized events were marked by the recognition system.**

***Index Terms*—Deception Island, hidden Markov modeling (HMM), seismic-event classification, volcano monitoring.**

I. Introduction

SEISMIC SIGNALS generated in volcanic areas display a broad range of characteristics and have been classified in different groups [e.g., volcano-tectonic (VT) earthquakes, long period (LP) events, volcanic tremor, or hybrid events]. These types of signals are related to different source processes, from the brittle response of a rock under stress as VT to the resonance of a conduit or crack due to the presence of fluids in movement as LP or tremor. The state of a volcano and the vicinity of a possible eruption can be controlled by analysis of these seismic signals [1], [2].

Monitoring of precursory seismicity in restless volcanoes is the most reliable and widely used technique in volcano monitoring [1]. The rate of occurrence of seismicity in an active volcano is high, with the presence of hundreds of events per hour in days or weeks. Each seismic event is related to different source processes. In order to understand the current state of the volcano, we should identify these processes. For this reason, the conclusive identification of the signal is a primary and critical point in volcano monitoring. In a crisis situation, there is a need to make fast decisions, which can affect public safety. Based on the number and type of seismic events, analysts working in volcanic observatories have to decide the protocol to follow near real time. In many situations, a visual classification on the sole basis of the seismogram appearance may be the only way to discriminate between internal volcanic earthquakes and external or nonnatural signals. A more detailed analysis, including, e.g., spectral characteristics, would be too time consuming to be carried out in real time. The development of a robust automatic discrimination algorithm helps the analysis, enabling technicians to focus their efforts on the interpretation of the situation or to analyze only a reduced number of signals.

Recently, Del Pezzo *et al.* [3] and Scarpetta *et al.* [4] have presented the application of neuronal networks for discrimination and classification of volcanic and artificial signals at the Vesuvius Volcano and Phlegraean Fields, Italy. These methods have been successfully applied to discriminate signals for local and volcanic seismicity. A serious limitation of these systems is that they require previous inspection of the data in order to extract a collection of events of the same duration from the continuous recorded signal. In this paper, we advance in the field and develop a continuous seismic-event recognition and monitoring system that is based on the state of the art of hidden Markov model (HMM)-based pattern recognition techniques successfully applied to other disciplines such as robust automatic speech recognition (ASR) systems. One of the main advantages of our system over Del Pezzo's method [3] is that it is able to work in continuous mode over real-time recordings and recognize volcanic events occasionally found in LPs of just background seismic noise. On the other hand, our system detects events on a noisy signal and discriminates between four different types of seismic events, namely: 1) LP; 2) earthquake; 3) hybrid; and 4) volcanic tremor, while Del Pezzo's system considers only a two-class classification problem for earthquakes and underwater explosions.

HMMs are a powerful tool in modeling any time-varying series. Ornhberger [5] has studied discrete HMM tools for continuous seismic-event classification. As in continuous speech modeling, where the signals are modeled as a concatenation of different acoustic events (e.g., phone and words), seismic records can be also modeled as a time sequence of different seismic events. Furthermore, different realizations of the same seismic event have similar spectral patterns. Fig. 1 shows two different hybrid events registered at Deception Island, Antarctica. Note that the spectrograms have similar spectral components and that both hybrid events exhibit the

Manuscript received November 4, 2005; revised April 24, 2006. This work was supported in part by the Spanish Government under TEIDEVS (CGL2004-05744-C04-01/BTE) project and in part by European Commission under EU/VOLUME project.

M. C. Benítez, J. Ramírez, J. C. Segura, and G. Cortés are with the Departamento de Teoría de la Señal Telemática y Comunicaciones, University of Granada, 18071 Granada, Spain (e-mail: javierrp@ugr.es).

J. M. Ibáñez, J. Almendros, and A. García-Yeguas are with the Instituto Andaluz de Geofísica, University of Granada, 18071 Granada, Spain.

Digital Object Identifier 10.1109/TGRS.2006.882264

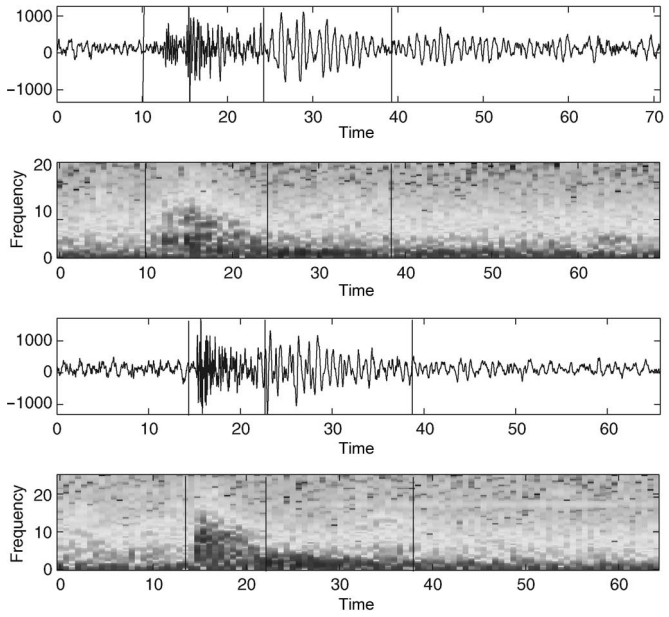

Fig. 1. Two different hybrid events recorded at Deception Island during 1994–1995.

same instantaneous behavior; thus, they are suitable to be modeled by HMMs.

A. Deception Island

The data used in this paper were recorded from the Deception Island Volcano, Antarctica, during three summer Antarctic surveys during 1994–1995, 1995–1996, and 2001–2002. The data set consists of thousands of seismic events that contains VT earthquakes, LP events, hybrids, and tremor. Fig. 2 shows the location of the island and the placement of the seismic arrays. Deception Island is a volcanic island located at $62^\circ\,59'$ S and $60^\circ\,41'$ W in the South Shetland Islands region. This island is a back-arc stratovolcano. The basal diameter of the island is 30 km and rises 1400 m from the seafloor to a maximum height of 540 m above sea level. The 15-km-diameter island is horseshoe-shaped and displays a flooded caldera (Port Foster) with dimensions of 6×10 km and a maximum depth of 190 m. The caldera wall is breached by a 500-m-wide passage called Neptune's Bellows. Glaciers cover almost half of the island, mainly on Mount Pond and Mount Kirkwood in the east and south, respectively.

It is the main active volcano of the Bransfield Strait, a northeast (NE)-trending series of basins located between the South Shetland Islands arc and the northwestern tip of the Antarctic Peninsula [6], [7]. This region represents one of the major known sites of seismic and volcanic activity in Antarctica. Deception Island is the most active of all the volcanoes in the South Shetland Islands, having erupted at least six times since it was first visited 160 years ago [8], [9]. All historical eruptions were relatively small in volume and occurred at locations near the coast of the inner bay. Three eruptions between 1967 and 1970 were observed directly and are well documented [10], [11]. In December 1967, two eruptions developed simultaneously from sites that are located 2 km apart. One of them was a submarine eruption that gave rise to a new island in Telefon Bay, while the other occurred inland, between Telefon Bay

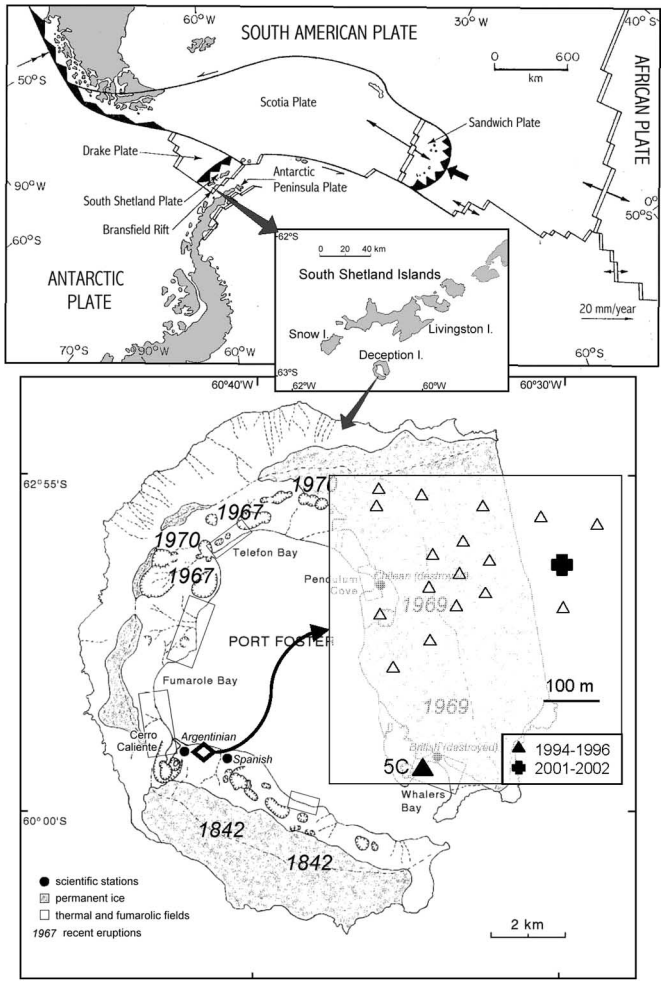

Fig. 2. Map of Deception Island and the configuration of the instruments used in the data analysis. In the upper figure, we show the geographical situation of the Deception Island Volcano in the South Shetland Islands, Antarctica. In the map, we marked the main volcanic features, including dates of recent historical eruptions.

and Pendulum Cove. In both cases, the eruptive products were similar (ash, steam, and some bombs), but the Telefon second eruption occurred in February 1969, when fissures opened in the ice on the west-facing slopes of Mount Pond, which are accompanied by pyroclastic emissions. The last eruption was in August 1970, when additional activity along the northern edge of Telefon Bay formed a chain of new craters and modified the coastline. Evidence of the present-day volcanic activity at Deception Island includes fumarolic activity, hydrothermal areas, resurgence of the floor of Port Foster, and seismicity [12]–[15]. Fumaroles and hot springs with temperatures of below 110 °C encircle Port Foster [16].

B. Data Acquisition

The data analyzed in this paper were recorded in the Deception Island Volcano by a dense short-period seismic antenna that operated during the 1994–1995 and 1995–1996 summer field surveys, and a three-component autonomous seismic station during the 2001–2002 survey. These surveys spanned from December to February. The seismic antenna was located between the Argentinean and Spanish Stations (Fig. 2) and was composed of 3 three-component and 15 vertical seismometers.

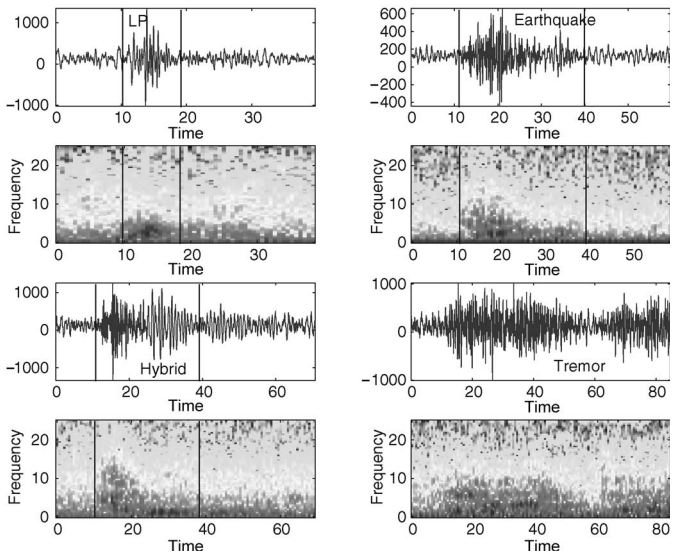

Fig. 3. Spectral characteristics of seismic events recorded at Deception Island.

The vertical seismometers were Mark L25, with a natural frequency of 4.5 Hz. Their response was electronically extended to 1 Hz. The 3-D seismometers were Mark L-4C with a natural frequency of 1 Hz. The preamplifier's output is balanced so that the signal is sent undisturbed via twisted-pair cables to the data-acquisition system. The array structure is based on eight-channel modules. Three of such modules composed the whole seismic antenna. Each data-acquisition module has the following components: an eight-channel antialias Butterworth multipole filter at 48 Hz, a multiplexer that samples each of the eight channels every 5 ms, and a 16-bit analog-to-digital (A/D) converter. The internal clock is synchronized by GPS time every second, and the sampling rate used is 200 sample/s. The control of each module and the storage of the data are done by a portable personal computer. The triggering algorithm is based on the short-term average/long-term average (STA/LTA) ratio. The three-component station was located near the Spanish Station. The sensors used were Mark L-4C and were connected to a data-acquisition system with a resolution of 24 bits and a sampling rate of 50 sample/s. While the array recorded data by triggering, this autonomous station was set in a continuous recording mode.

C. Data Characteristics

The seismicity recorded at Deception Island is grouped in the following categories: local VT earthquakes, LP events, hybrid events, and volcanic tremor. The characteristics of this seismicity have been widely studied using different techniques, as reported in [13] and [25]. Fig. 3 shows the spectral characteristics of the different kinds of events, which are characterized as follows.

1) LP events recorded at Deception Island are signals with a fuse-shaped envelope with a duration of less than 60 s and almost pure monochromatic spectral content at frequencies of below 4 Hz. In some cases, a high-frequency phase precedes some of these events. They are related to resonances of fluid-filled conduits and cracks that are driven by volcanic processes.
2) Local VT events are earthquakes with S-P waveform time shorter than 4 s. This time limit ensures that the VT events are located inside the island structure. They are usually characterized by impulsive direct P and S wave arrivals. The spectral content of this signal is very broad, reaching up to 30 Hz. The source of these local VT earthquakes can be interpreted as the brittle response of the volcanic environment under local and regional stresses. The origin of these stresses is related to volcanic processes within the island and varies from the interaction of water with hot materials to the effects of shallow magma injections.
3) Hybrid events are signals that contain both double-couple and volumetric components. They are characterized by an initial high-frequency phase, which corresponds to a VT earthquake in which P and S waves might be distinguished, followed by a monochromatic signal that is similar to those shown by the LP events. In some cases, LP events with an energetic initial high-frequency signal can be interpreted as hybrids.
4) Volcanic tremor is a monochromatic signal with a duration that is longer than that observed for LP events. Episodes of tremor that vary from minutes to several hours and days have been observed. Tremor and LP events are different manifestations of the same process. An LP event is the response to a sudden pressure transient within a fluid-filled crack, while a tremor is the response to continuous fluctuation of pressure.

II. HMM-Based Seismic-Event Modeling

The basic theory of HMMs was published in [17] and [18] in the late 1960s. The first application in speech recognition was developed in the early 1970s by Baker [19] at Carnegie Mellon University (CMU), and Jelinek [20] and Jelinek and Bahl [21] at IBM. HMMs [22] can be used to model any time series. There are two major processing stages involved in an HMM-based pattern recognition system. First, the training algorithms are used to set the parameters of the HMMs by means of a database that contains seismic recordings and their associated transcriptions. Second, unknown seismic records are transcribed using the decoding algorithms [23], [24]. This section shows the general principles of HMMs and the theoretical background for seismic-event recognition.

A. Definition

An HMM-based seismic-event recognition system must assume that the signal is a realization of a sequence of one or more symbols. In order to perform the recognition process, the recognizer decomposes the incoming signal as a sequence of feature vectors. This sequence is assumed to be a precise representation of the seismic signal, while the length of the analysis window is such that the seismic waveform can be considered as stationary.

The goal of the recognition system is to perform a mapping between a sequence of feature vectors and the corresponding sequence of seismic events. The main obstacles associated with this task that strongly affect the system performance are the variability of the seismic events, the propagation between the source and the seismic registration stations, and the noise sources that are present in the environment. Another drawback

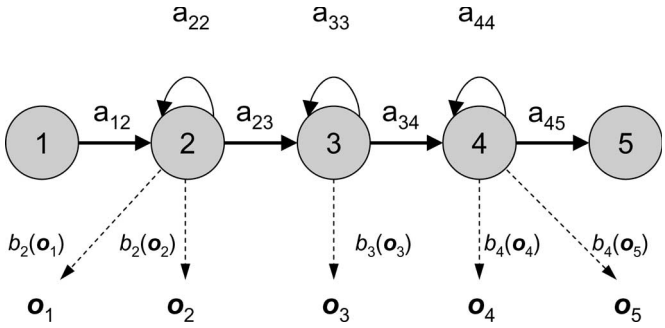

Fig. 4. Five-state left-to-right HMM with nonemitting entry and exit states.

is that the boundaries between symbols cannot be identified explicitly. This problem can be avoided by restricting the task to isolated event recognition. The simplified problem serves as a good basis for introducing the basic ideas of HMM-based pattern recognition, while the main objective of this paper is the development of a continuous seismic-event classification and monitoring system.

B. Seismic-Event Recognition

Let a sequence of seismic events $\mathbf{w} = w_1, w_2, \ldots, w_l$ be represented as a sequence of feature vectors $\mathbf{o}_t$ or observations $\mathbf{O}$, which is defined as

$$\mathbf{O} = \mathbf{o}_1, \mathbf{o}_2, \ldots, \mathbf{o}_t \tag{1}$$

where $\mathbf{o}_t$ is the signal vector observed at time t. The solution to the problem of continuous event recognition is selection of the sequence of events $\mathbf{w}$ with the maximum probability $P(\mathbf{w}|\mathbf{O})$, i.e.,

$$\arg\max_{\mathbf{w}} P(\mathbf{w}|\mathbf{O}). \tag{2}$$

Using Bayes' rule, we have

$$P(\mathbf{w}|\mathbf{O}) = P(\mathbf{O}|\mathbf{w})P(\mathbf{w})/P(\mathbf{O}). \tag{3}$$

In almost any given application scenario, the dimensionality of the feature vectors does not make the estimation of the joint conditional probability $P(\mathbf{o}_1, \mathbf{o}_2, \ldots, \mathbf{o}_t)$ from examples practicable. If a parametric model for seismic-event production such as a Markov model is assumed, the problem is reduced to estimating the Markov-model parameters. The objective then is to analyze the incoming signal consisting of a large sequence of nondelimited seismic events and recognize the corresponding sequence of events. The next section addresses the development of a continuous recognition system for seismic events of volcanic origin.

C. HMMs

HMM-based pattern recognition systems normally assume that the sequence of observed feature vectors corresponding to each event is generated by a Markov model. A Markov model is essentially a finite-state machine with several states. Fig. 4 shows a five-state left-to-right HMM with nonemitting entry and exit states. A change of state takes place every time unit, and a feature vector $\mathbf{o}_t$ is generated from a probability density $b_j(\mathbf{o}_t)$ that is determined during the training process. Moreover,

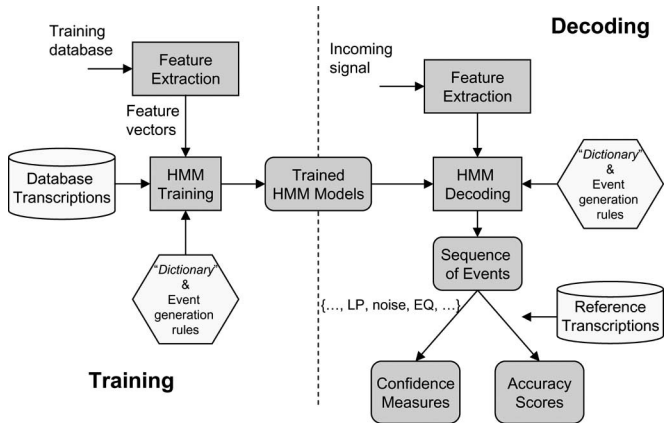

Fig. 5. Architecture of an HMM-based seismic monitoring system.

the transition from state i to state j is governed by the transition probabilities a_{ij}, which are used to model the delay in each of the states and the transitions through the entire model. Thus, the joint probability that observation $\mathbf{O}$ generated by using models M_i is calculated, summing all possible state sequences $\mathbf{X} = x(1), x(2), \ldots, x(T)$, i.e.,

$$P(\mathbf{O}|M_i) = \sum_X a_{x(0)x(1)} \prod_{t=1}^{T} b_{x(t)}(\mathbf{o}_t) a_{x(t)x(t+1)}. \tag{4}$$

The underlying method for statistical pattern recognition assumes that the parameters of models M_i is known. These parameters are obtained given a number of training examples and their associated transcriptions by means of efficient reestimation procedures. In order to recognize some unknown event, the likelihood of each model generating that event is calculated, and the most likely model identifies the event. On the other hand, the specification of output probabilities $b_j(\mathbf{o}_t)$ is normally based on a parametric model. For instance, in speech recognition applications, a widely used representation is by means of Gaussian mixture densities.

D. HMM-Based Seismic-Event Recognition System

Fig. 5 shows the architecture of a general-purpose HMM-based pattern recognition system. The training database and transcriptions are used to build the models. Once the models are initiated, the recognition system performs feature extraction and decoding based on the Viterbi algorithm. The output is the sequence of recognized events, confidence measures, and global accuracy scores.

III. Preliminary Data Preparation

A. Seismic-Data Preprocessing

In the actual implementation of the recognition system, it is not possible to accept the seismic signal in the format that was created for the array and based on multiplexed signals. The input signal for both training and recognition is a stream of 16-bit binary data without a heading. Fig. 6 shows a hybrid event that was registered at Deception Island during the 1995–1996 field survey. It is shown that the energy of the signal is concentrated at frequencies of below 20 Hz. As the seismic-event recognition

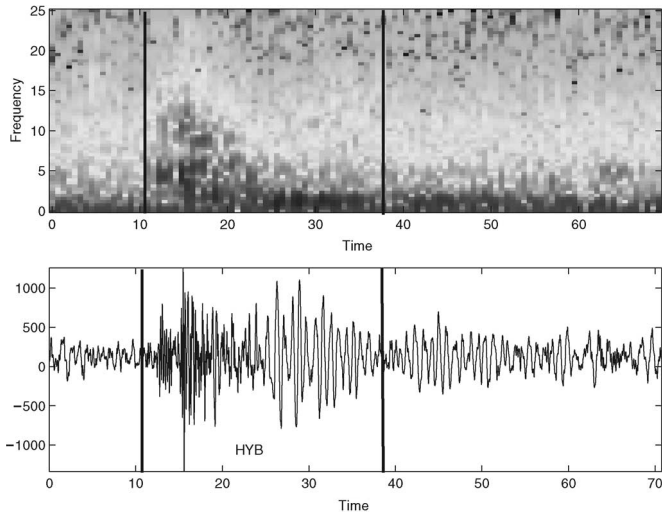

Fig. 6. Labels assigned to the seismic data for training.

system is based on the spectral properties of the signals, recordings that were initially sampled at 200 Hz were decimated to a 50-Hz sample rate using a 101-tap linear-phase finite-impulse response (FIR) filter. Two advantages are then obtained. First, redundant information, which does not contribute to a clear identification of the different events, is removed. Second, the computational cost of the recognition system is reduced.

B. Collecting the Training Database

As observed from Fig. 2, the seismic array is composed by 24 different channels. In order to perform the data analysis, we have selected channel number 5C, as shown in Fig. 2. We assume that the distance among the different stations is too small to produce differences between seismic stations. However, the local geology below each seismometer affects slightly the signal shape. Based on previous seismological works [13], [25], we have determined that this channel presented the signal with the highest signal-to-noise ratio (SNR).

The training process of the signal was performed in the three steps.

- Step 1) Visual recognition. The signal was analyzed on the screen of the computer, and its shape was compared with the description of the signals performed by Ibáñez *et al.* [13].
- Step 2) Spectral shape. Those signals that could be mixed in different sets were analyzed, observing their spectrogram.
- Step 3) Based on both criteria, each signal was labeled as "LP," "EQ," "HYB," "TREMOR," or "NOISE" to denote LP, earthquake, hybrid, or tremor events, or just seismic noise. The duration of the signal was established in the time domain inspecting the seismic waveform.

IV. Seismic-Event Recognition System

A. Feature Extraction

The first step of the recognition process is signal processing feature extraction, which converts the volcano seismic waveform to a parametric representation with less redundant information for further analysis and processing. As the short-time spectral envelop representation of the signal has been widely used, with good results, in speech recognition systems [26], a similar representation for our volcano seismic recognition system is used in this paper.

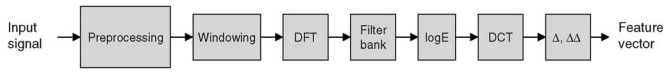

Fig. 7. Feature extraction.

Fig. 7 shows a block diagram of the feature extraction process, which is based on a filter-bank spectrum-analysis model. The signal is arranged into 4-s overlapping frames with a 0.5-s frame shift using a Hamming window. A 512-point fast Fourier transform (FFT) is used to compute the magnitude spectrum, which serves as the input of an emulated filter bank that consists of 16 triangular weighting functions that were uniformly spaced between 0 and 20 Hz. The overlap between adjacent filters is 50%. The purpose of the filter-bank analyzer is to give a measurement of the energy of the signal in a given frequency band. Then, the natural logarithm of the output filter-bank energies is calculated, resulting in a 16-parameter feature vector. Since the log filter bank energies are highly correlated and the recognition system uses continuous observation HMMs with diagonal covariance matrices, it is necessary to apply a decorrelation transformation. Thus, the discrete cosine transform (DCT) is used to decorrelate the features and reduce the number of components of the feature vector from 16 to 13 coefficients. Finally, the feature vector is augmented with linear regressions of the features (derivatives and accelerations), obtaining a total of 39 parameters.

B. Recognition System

The recognition system presented in this paper is based on continuous HMMs (CHMMs). CHMMs are trained for each event (earthquake, LP, hybrid, and tremor events), and a noise model is used to represent sequences with no events. Both training and recognition processes are performed using the HMM Tool Kit (HTK) software [27].

In a CHMM, the emission probabilities previously defined in Section II $b_{x(t)}(\mathbf{o}_t)$ for a feature vector $\mathbf{o}_t$ in state $x(t)$ are given by

$$b_{x(t)}(\mathbf{o}_t) = \prod_{s=1}^{S} \sum_{k=1}^{K} c_{\mathrm{sk}} \mathrm{N}(\mu_k, \sigma_k, \mathbf{o}_t) \tag{5}$$

where S is the number of parameters in the feature vector and K is the number of probability density functions (pdfs) considered. It is worthwhile clarifying that multivariate Gaussian pdfs with diagonal covariance matrices are used in this paper.

The training algorithm for the HMM consists of finding the parameters of the model (i.e., the weights for each state of the HMM c_{sk} and the transition probabilities between states a_{ij} of the model) from a previously labeled training database. Usually, the maximum-likelihood criterion is chosen as the estimation function to adjust the model parameters, i.e., the maximization of $P(\mathbf{O}|M)$ over M, where M defines an HMM. However, there is no known way to obtain a solution in a closed form. The Baum–Welch algorithm [28], [29] is an iterative procedure that provides a locally optimum solution to solve this problem.

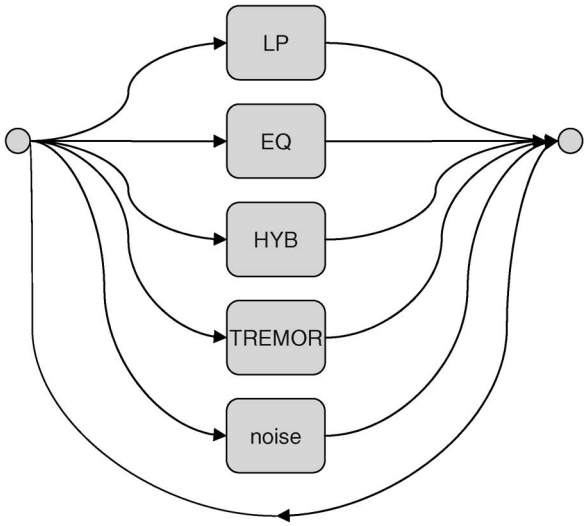

Fig. 8. Allowed sequence of recognized seismic events.

In the training process, it is necessary to fix the following:

1) topology of the models (in this case, classical left-to-right HMMs, as shown in Fig. 4, were used);
2) number of states for the models;
3) number of multivariate Gaussian pdfs;
4) number of iterations of the Baum–Welch algorithm.

The operation of the recognition system is described in (3), which allows to express $P(\mathbf{w}|\mathbf{O})$ in terms of computable magnitudes. Note that $P(\mathbf{O}|\mathbf{w})$ is the conditional probability of vector sequence $\mathbf{O}$, given the sequence of events $\mathbf{w}$, which can be computed by the HMMs, while $P(\mathbf{w})$ is the probability of the sequence of events $\mathbf{w}$.

As there is no statistical knowledge of possible event sequences, we assume that after a particular event, any other event or noise could appear with the same probability. Fig. 8 shows the transition rules between events that were considered in this paper.

The recognition process combines the probabilities generated by the models and the probabilities obtained by the allowed transition for the seismic events. Equation (2) indicates that it is necessary to generate all the possible sequences of events and to evaluate all of them using (3), thus selecting the one with the maximum probability. There are several algorithms to expand and search the most probable sequence of events, given a sequence of observations. The most popular algorithms used for speech recognition are stack decoding [28] and Viterbi search [30]. Among them, Viterbi decoding [26], [27], [31] is adopted in this paper. Additional details of the implementation of the training and decoding processes are provided.

1) Initial flat models are generated as HMM prototypes using the training database.
2) The Baum–Welch reestimation algorithm is performed using the training database, which includes the labeled seismic records. The number of iterations of the Baum–Welch algorithm is fixed to 6.
3) Initial HMMs are obtained with one multivariate Gaussian pdf.
4) The number of multivariate Gaussian pdfs is increased from 1 to 24. The reestimation algorithm is performed in each iteration, as in step 2), and recognition results using the Viterbi algorithm are obtained in each step.

TABLE I
RECOGNITION ACCURACY FOR DIFFERENT NUMBERS OF STATES N_E AND NUMBERS OF GAUSSIANS N_G

$N_E \backslash N_G$	4	8	12	16	20	24
9	61.89	70.65	74.77	79.30	81.46	83.11
11	74.15	82.29	84.65	87.23	89.29	91.04
13	76.31	81.57	84.76	86.71	88.67	89.50
15	73.94	81.15	84.14	86.41	86.82	87.95
17	74.56	79.40	81.26	83.32	84.45	85.38

V. EXPERIMENTAL RESULTS

The training database consists of 512 manually labeled, 150-s-long records that contain four classes of events, as discussed in Section I. It includes: 1) 75 local VT earthquake events (EQ); 2) 765 LP events (LP); 3) 54 hybrid events (HYB); and 4) 77 volcanic tremor events (TREMOR).

The experimental results are shown in Table I. These results are obtained for the whole training database. The performance of the system is given in terms of the recognition accuracy that is defined as

$$\mathrm{Acc}(\%) = \frac{C - I}{N} \times 100\% \tag{6}$$

where C is the number of correctly recognized events, I is the number of insertion errors, and N is the total number of events present in the test. Table I shows the accuracy values for a variable number of Gaussians (4–24) when the number of states of the models varies from 9 to 17. It can be observed that the performance of the system increases with the number of Gaussians used to model each state of the HMMs; the upper bound depends on the size of the training database. The best results are obtained when the events are modeled with 11 states, yielding accuracy values of up to 90%. Note that the number of states of the models imposes a minimum duration for the events. In this paper, 4-s analysis frames with a 0.5-s frame shift were used. Thus, for the topology of the HMMs adopted in this paper, the minimum duration that the system assigns to an event is obtained by multiplying the number of states by the frame shift (0.5 s). Fig. 9 shows the histogram of the length of events that appear in the training database; only 8.5% of the events (LP events) present a length that is less than 5.5 s; for this reason, the best tradeoff obtained for this particular database is 11 states.

It is worthwhile clarifying several issues regarding this preliminary set of experiments. Our data set consists of recordings for four types of seismic events: VT earthquakes, LP, hybrid, and volcanic tremor events; each class is defined by means of a trained HMM that models its time-varying power spectral pattern. In order to train each model accurately, a large number

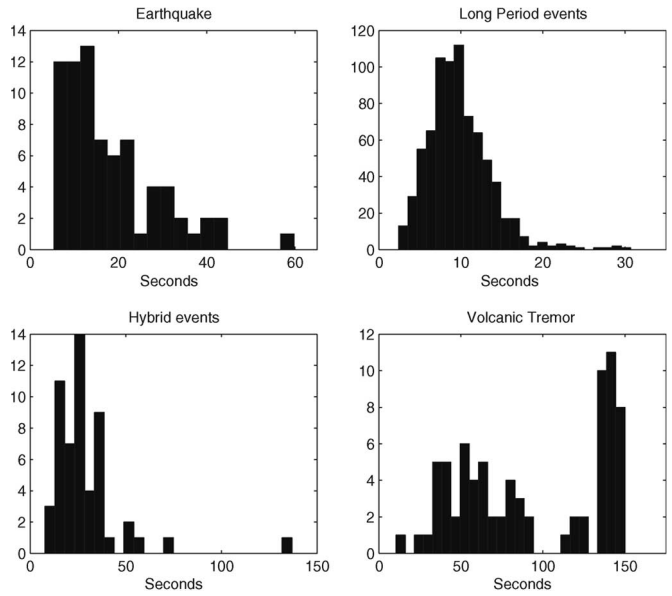

Fig. 9. Histogram of the length of the events present in the training database.

of occurrences belonging to the same class in the training data set is needed. In case of a limited data set, it is not effective to split the data set into two different disjoint data sets for training and testing since the HMMs for events with a reduced number of occurrences in the training data set will not be accurately estimated. Only for LP events, the number of realizations is large enough to proceed with this strategy. In order to solve this drawback, we have adopted a technique that is frequently used in HMM-based pattern recognition systems when only a limited database is available for training and testing. The strategy known as "leave one out" [32] consists of conducting multiple training and testing experiments with different partitions of the database for training and testing and of averaging the results of these tests. With this method, we have validated the results shown in Table I with a low degradation of the system performance from that obtained for the previous experiment.

The confusion matrices are useful to better describe the three kinds of mistakes that appear in the automatic recognition system: substitution errors, insertion errors, and deletion errors. Table II shows four confusion matrices for different experiments with 16 Gaussians and 9, 11, 13, and 15 states. In all the cases, the confusion matrix is almost diagonal. Reading across the rows of the confusion matrix, each column represents the number of times that the event was automatically labeled by the system as such event. For example, Table II(a) shows that 707 times were the LP events recognized as LP, 3 times as EQs, and 7 times as TREMOR; the recognition system was not able to identify the event 48 times. The "Ins" row indicates the number of times that each one of the events was incorrectly detected when just noise is present in the signal. Note that the number of LP events in the database is considerably greater than the rest of the events. The selection of the number of states affects especially this type of event, which is better recognized with $N_E = 11$ states. According to the histograms shown in Fig. 9, for an increasing number of states, the number of LP deletion errors increases with the corresponding reduction of the number of insertion errors.

A. Additional Tests of the Recognition System

In order to control the accuracy of the recognition method with other signals that were not used in the training process, we selected the data recorded in the 2001–2002 field survey by the autonomous seismic station. In this period, several seismic swarms were recorded, with durations ranging from hours to days. During the routine study performed in the field, a selection of the whole data set, which contains thousands of events, mainly LP events, was done. Unfortunately, the moderate volcanic activity in the island during the field survey showed that no other types of seismic event different from LP events were observed. This new data set has been used to control the recognition method. The result of the application of the recognition process to this data set reveals a great success, as summarized in the following list.

1) No other type of signal was recognized, and only LP events were marked.
2) The seismic noise was recognized as noise, although the nature and amplitude of the noise were different between the training database and the testing one.
3) More than the 95% of the recognized LP events were marked by the recognition process.
4) The recognition process marked other signals as LP events, which initially did not appear to be classified as that in the database. After a spectral analysis, we observed that they also should be classified as LP, but they were not labeled as events due to their low amplitude.

Finally, preliminary results of a direct comparison between the proposed HMM-based system and Del Pezzo's method [3] are given. Having clarified in Section I that both systems are different and perform different tasks on the seismic signal, we have obtained preliminary results for the comparison of both methods. Thus, direct evaluation of the system presented in this paper with the data set used to evaluate the system by Del Pezzo *et al.* [3] shows that the system proposed by Del Pezzo [3], which is based on neuronal networks, yielded a 90% classification accuracy for a task consisting of classifying earthquakes and underwater explosions at Phlegraean Fields, while our HMM-based recognition system reported a 97% recognition accuracy for the same task.

VI. Conclusion

Monitoring of precursory seismicity in restless volcanoes is the most reliable and widely used technique in volcano monitoring. This paper showed a complete seismic-event recognition and monitoring system that is based on the state of the art in HMM successfully applied to other disciplines including ASR systems. A database that contains a representative set of different seismic events including VT earthquakes, LP events, volcanic tremor, or hybrid events was collected from Deception Island for training and testing. Simple left-to-right HMMs and multivariate Gaussian densities with a diagonal covariance matrix were used. The feature vector includes the log-energies of a filter bank that consists of 16 triangular weighting functions that were uniformly spaced between 0 and 20 Hz and the first- and second-order derivatives. The system is suitable to operate in real time and capable of discriminating between different types of seismic events with an accuracy of about 90%. On the other hand, when the system was tested with a different data

TABLE II
CONFUSION MATRICES. (a) $N_E = 9$ STATES. (b) $N_E = 11$ STATES. (c) $N_E = 15$ STATES. (d) $N_E = 17$ STATES

	LP	HYB	EQ	TREMOR	Del
LP	707	0	3	7	48
HYB	0	53	0	0	1
EQ	5	0	69	0	1
TREMOR	5	0	0	72	0
Ins	63	4	4	60	

(a)

	LP	HYB	EQ	TREMOR	Del
LP	696	0	1	4	64
HYB	0	54	0	0	0
EQ	1	0	73	0	1
TREMOR	2	0	0	73	2
Ins	35	0	0	14	

(b)

	LP	HYB	EQ	TREMOR	Del
LP	675	0	1	3	86
HYB	0	54	0	0	0
EQ	3	0	71	1	0
TREMOR	3	0	0	73	1
Ins	24	0	0	7	

(c)

	LP	HYB	EQ	TREMOR	Del
LP	653	0	0	4	108
HYB	0	54	0	0	0
EQ	3	1	69	0	2
TREMOR	4	0	0	72	1
Ins	29	0	0	10	

(d)

set that is composed mainly of LP events, more than 95% of the recognized events were marked correctly by the recognition system. Thus, the system enables monitoring the state of a volcano and the vicinity of a possible eruption by analyzing these seismic signals. As a conclusion, the system developed in this paper is very useful in discriminating among different types of volcanic signals after a careful training process. With this valuable tool, analysts working on many volcanic observatories can decide in near real time the protocol to follow based on the number and type of seismic events.

ACKNOWLEDGMENT

The authors would like to thank E. Del Pezzo and S. Scarpetta for providing the data set recorded at Phlegraean Fields, which was used for a preliminary comparison between their system and the proposed HMM-based system. The authors would also like to thank the anonymous reviewers for their helpful comments, which have contributed in enhancing this paper.

REFERENCES

[1] B. Chouet, "New methods and future trend in seismological volcano monitoring," in *Monitoring and Mitigation of Volcano Hazards*. New York: Springer-Verlag, 1996, pp. 23–97.

[2] ——, "Volcano seismology," *Pure Appl. Geophys.*, vol. 160, no. 3/4, pp. 739–788, 2003.

[3] E. Del Pezzo, A. Esposito, F. Giudicepietro, M. Marinaro, M. Martini, and S. Scarpetta, "Discrimination of earthquakes and underwater explosions using neural networks," *Bull. Seismol. Soc. Amer.*, vol. 93, no. 1, pp. 215–223, Feb. 2003.

[4] S. Scarpetta, F. Giudicepietro, E. Ezin, S. Petrosino, E. Del Pezzo, M. Martini, and M. Marinaro, "Automatic classification of seismic signals at Mt. Vesuvius volcano, Italy, using neural networks," *Bull. Seismol. Soc. Amer.*, vol. 95, no. 1, pp. 185–196, Feb. 2005.

[5] M. Ohrnberger, "Continuous automatic classification of seismic signals of volcanic origin at Mt. Merapi, Java, Indonesia," Ph.D. dissertation, Math.-Naturwissen. Facultat der Univ. Potsdam, Potsdam, Germany, 2001.

[6] M. Grad, A. Guterch, and P. Sroda, "Upper crustal structure of Deception Island area, Bransfield Strait, West Antarctica," *Antarct. Sci.*, vol. 4, no. 4, pp. 469–476, 1992.

[7] D. Barker and J. Austin, "Rift propagation, detachment faulting, and associated magmatism in Bransfield Strait, Antarctic Peninsula," *J. Geophys. Res.*, vol. 103, no. B10, pp. 24017–24043, Oct. 1998.

[8] O. Gónzalez, *Volcanes de Chile*. Argentina: Inst. Geogr. Militar, 1995.

[9] C. Newhall and D. Dzurisim, "Historical unrest at large calderas of the world," in *U.S. Geol. Surv. Bull.*, vol. 1/2, 1988.

[10] J. Smellie, "Recent observations on the volcanic history of Deception Island, South Shetland Islands," in *Br. Antarct. Surv. Bull.*, vol. 81, 1988, pp. 83–85.

[11] P. Baker, I. McReath, M. Harvey, M. Roobol, and T. Davis, "The geology of the South Shetland Islands: Volcanic evolution of Deception Island," in *Br. Antarct. Surv. Sci. Reports*, 1975, pp. 78–81.

[12] A. Cooper, J. Smellie, and J. Maylin, "Evidence for shallowing and uplift from bathymetric records of Deception Island, Antarctica," *Antarct. Sci.*, vol. 10, no. 4, pp. 455–461, 1998.

[13] J. Ibáñez, E. Del Pezzo, J. Almendros, M. L. Rocca, G. Alguacil, R. Ortiz, and A. García, "Seismo volcanic signals at Deception Island Volcano (Antarctica): Wavefield analysis and source modeling," *J. Geophys. Res.*, vol. 105, no. 6, pp. 13905–13931, 2000.

[14] R. Ortiz, J. Vila, A. García, J. González, J. Diez, A. Aparicio, R. Soto, J. G. Viramonte, C. Risso, and I. Petrinovic, "Geophysical features of Deception Island," in *Recent Progress in Antarctic Earth Science*. Tokyo, Japan: Terra Scientific, 1992, pp. 143–152.

[15] J. Rey, L. Somoza, and J. Martínez, "Tectonic, volcanic, and hydrothermal event sequence on Deception Island (Antarctica)," *Geo-Mar. Lett.*, vol. 15, no. 1, pp. 1–8, Mar. 1995.

[16] J. Smellie, "Deception Island," in *Volcanoes of the Antarctic Plate and Southern Oceans*. Washington, DC: Amer. Geophys. Union, 1990, pp. 316–321.

[17] L. Baum and T. Petrie, "Statistical inference for probabilistic functions of finite state Markov chains," *Ann. Math. Stat.*, vol. 37, no. 6, pp. 1554–1563, 1966.
[18] L. Baum, T. Petrie, G. Soules, and N. Weiss, "A maximization technique ocurring in the statistical analysis of probabilistic functions of Markov chains," *Ann. Math. Stat.*, vol. 37, no. 1, pp. 1554–1563, 1970.
[19] J. Baker, "The dragon system—An overview," *IEEE Trans. Acoust., Speech Signal Process.*, vol. ASSP-23, no. 1, pp. 24–29, Feb. 1975.
[20] F. Jelinek, "A fast sequential decoding algorithm using a stack," *IBM J. Res. Develop.*, vol. 13, no. 6, pp. 675–685, 1969.
[21] L. Bahl and F. Jelinek, "Decoding for channels with insertions, deletions, and substitutions with applications to speech recognition," *IEEE Trans. Inf. Theory*, vol. IT-21, no. 4, pp. 404–411, Jul. 1975.
[22] L. Rabiner, "A tutorial on hidden Markov models and selected applications in speech recognition," *Proc. IEEE*, vol. 77, no. 2, pp. 257–286, Feb. 1989.
[23] A. Viterbi, "Error bounds for convolutional codes and asymptotically optimal decoding algorithm," *IEEE Trans. Inf. Theory*, vol. IT-13, no. 2, pp. 260–269, Apr. 1967.
[24] G. Forney, "The Viterbi algorithm," *Proc. IEEE*, vol. 61, no. 3, pp. 268–278, Mar. 1973.
[25] C. Martinez-Arevalo, F. Bianco, J. Ibáñez, and E. Del Pezzo, "Shallow seismic attenuation and shear waves splitting in the short period range of Deception Island Volcano (Antarctica)," *J. Volcanol. Geotherm. Res.*, vol. 128, no. 1, pp. 89–113, Nov. 2003.
[26] L. Rabiner and B. Juang, *Fundamentals of Speech Recognition*. Englewood Cliffs, NJ: Prentice-Hall, 1993.
[27] S. Young, J. Odell, D. Ollason, V. Valtchev, and P. Woodland, *The HTK Book*. Cambridge, U.K.: Cambridge Univ. Press, 1997.
[28] L. Bahl, F. Jelinek, and R. Mercer, "A maximum likelihood approach to continuous speech recognition," *IEEE Trans. Pattern Anal. Mach. Intell.*, vol. PAMI-5, no. 2, pp. 179–190, Mar. 1983.
[29] A. Dempster, N. Laird, and D. B. Rubin, "Maximum likelihood from incomplete data via the EM algorithm," *J. R. Stat. Soc.*, vol. 39, no. 1, pp. 1–38, 1977.
[30] K. F. Lee and H. W. Hon, "Large-vocabulary speaker-independent continuous speech recognition using HMM," in *Proc. Int. Conf. Acoust., Speech, Signal Process.*, 1988, vol. 1, pp. 112–126.
[31] S. Furui and M. M. Sondhi, *Advances in Speech Signal Processing*. New York: Marcel Dekker, 1992.
[32] K. Fukunaga, *Introduction to Statistical Pattern Recognition*. New York: Academic, 1990.

M. C. Benítez (M'91) received the M.Sc. and Ph.D. degrees in physics from the University of Granada, Granada, Spain, in 1988 and 1998, respectively.

Since 1990, she has been with the Department of Electrónica y Tecnología de Computadores, Faculty of Sciences, University of Granada, first as a Research and Assistant Professor and then as an Associate Professor since 2003. From 2001 to 2002, she was a Visiting Researcher with the International Computer Science Institute, Berkeley, CA. Her research interests include speech processing, with a specific goal of speech recognition, confidence measures, and robust parameterization for speech recognition.

Dr. Benítez is a member of International Speech Communication Association.

Javier Ramírez received the M.A.Sc. and Ph.D. degrees in electronic engineering from the University of Granada, Granada, Spain, in 1998 and 2001, respectively.

Since 2001, he has been an Assistant Professor with the Department of Signal Theory Networking and Communications, University of Granada. His research interest includes seismic signal processing, robust speech recognition, speech enhancement, voice activity detection and design, and implementation of high-performance digital signal processing systems, of which he has coauthored more than 100 technical journal and conference papers. He has served as a reviewer for several international journals and conferences.

José C. Segura (M'94–SM'03) was born in Alicante, Spain, in 1961. He received the M.S. and Ph.D. degrees in physics from the University of Granada, Granada, Spain, in 1984 and 1991, respectively. His Ph.D. dissertation was on a variant of hidden Markov modeling.

In 1986, he joined the Research Group on Signals, Networking, and Communications (GSTC), Department of Electronics and Computer Technology, University of Granada, where he was an Assistant Professor from 1987 to 1993 and has been an Associate Professor since 1993. He has also been the Coordinator of GTSC since January 2004. He has taught several national and international courses and directed three Ph.D. dissertations on topics related to speech recognition. His research interests include robust speech recognition, distributed speech recognition, and signal processing.

Dr. Segura is a member of the International Speech Communication Association and the Spanish Association for Pattern Recognition and Image Analysis.

Jesús M. Ibañez was born in Granada, Spain, in 1964. He received the M.Sc. degree in physics and the Ph.D. degree in seismology from the University of Granada, in 1987 and 1991, respectively.

Since 1993, he has been an Associate Professor with the University of Granada. Since 1999, he has been an Executive Secretary with the Instituto Andaluz de Geofísica, University of Granada. He has also worked for different universities such as Harvard University, Cambridge, MA; Catania University, Catania, Italy; and Salerno University, Salerno, Italy. He has directed several Ph.D. dissertations, published more than 60 Science Citation Index papers, and headed more than ten research projects on volcano seismology, working in different volcanoes around the world. His research interests include seismology, seismic attenuation, and volcano seismology.

Javier Almendros received the M.Sc. degree in physics (with specialization in astrophysics and geophysics) from the Universidad Complutense de Madrid, Madrid, Spain, in 1994 and the Ph.D. degree in physics, in the subject of volcano seismology, from the University of Granada, Granada, Spain, in 1999.

From 1999 to 2001, he was with the Volcano Hazards Team, U.S. Geological Survey. Since 2001, he has been a Research Fellow with the Instituto Andaluz de Geofísica, University of Granada, where he is involved in research and teaching. He also collaborates with several research groups in the study of different active volcanoes, as well as in the application and development of new tools and techniques for the analysis of seismo-volcanic data. His current research interests include volcano seismology.

Araceli García-Yeguas received the M.Sc. degree in physics from the University of Granada, Granada, Spain, in 2004. She is currently working toward the Ph.D. degree in volcano seismology at the University of Granada, where she works on seismic tomography of active volcanoes and problems related to seismic-wave propagation in heterogeneous media.

Guillermo Cortés was born in Granada, Spain. He received the M.S. degree in electronic engineering in 2004, from the University of Granada, Granada, where he is currently working toward the Ph.D. degree in multimedia technologies.

His research interests include geophysical software, pattern recognition, and multimodal processing.